International Journal of Engineering & Technology, 7 (4.39) (2018) 74-77

International Journal of Engineering & Technology

Website: www.sciencepubco.com/index.php/IJET

Research paper

Robust Fault Diagnosis for a Quadrotor with Actuator Fault

N.P. Nguyen[1], S.K. Hong[2*]

[1 2] Department of Aerospace Engineering, Sejong University, Seoul, South Korea
**Corresponding author E-mail: skhong@sejong.ac.kr*

Abstract

Background/Objectives: Fault diagnosis (FD) is a main role in active fault tolerant control system. It can not only determine the location but also estimate the magnitude of fault.
Methods/Statistical analysis: This article presents an adaptive fault diagnosis approach for a quadrotor with a simulated actuator fault. Firstly, the dynamics of the quadrotor are considered as a state space model. The magnitude of fault is identified through an adaptive law. Designed matrices and parameters are solving by linear matrix inequalities (LMI).
Findings: Unlike previous studies, the present method can determine time-varying actuator faults with disturbances consideration.
Improvements/Applications: Simulation results demonstrate that proposed method can estimate time-varying faults with high accuracy.

Keywords: *Quadrotorter, adaptive observer, sliding mode observer, fault estimation, fault diagnosis.*

1. Introduction

Quadrotor unmanned autonomous vehicles (UAVs) possess a wide range of advantages compared to other UAVs: hovering ability, simplicity, agility, maneuverability, working in dangerous environments, which have contributed to their increasing popularity in field applications.
The interest in Fault Tolerant Control (FTC) has dramatically increased over the past decades, which has contributed to the quadcopter UAVs being more reliable and safe during missions. Generally, in FTC systems, there are two methods: passive and active FTC. The Passive FTC does not require the fault diagnosis algorithm but it has a limitation of fault-tolerant capability[1]. Active FTC has been proposed which has not only resulted in an improved performance with regard to fault-tolerant capability, but also attracted an increasing number of researchers to the field of FTC. FD is essential to detect the locations and number of faults in active FTC and its results led to improved designs to alleviate the impact of these faults. Therefore, FD is the main role in the active FTC.
Several previous studies have examined FD in quadcopter UAVs. A model based on an observer approach is developed in [2] but this approach is not accurate and unsuitable for fault estimation. In[3], an adaptive observer based at H_∞ is presented to determine the amount of actuator fault. Although the algorithm showed some good results, it is not robust for unknown disturbances and the resulting model uncertainties, because the underlying mathematical model does not account for nonlinear terms and external disturbances. Ma and Zhang presented Kalman Filter algorithm for fault identification[4]. This study uses a linearization method for the nonlinear model which successfully simulates the system states and faults. However, KF-based fault diagnosis is of insufficient accuracy due to model uncertainties. A different method using an Adaptive Thau Observer (ATO) is presented in[5]. This studies applies identification techniques to compensate the drag terms which are considered as the uncertainties of quadrotor model. However, this method is time consuming because it does not consider external disturbances in the nonlinear model. In addition, several effective approaches toward FD such as neural networks[6], adaptive observers[7], and sliding mode observer[8] have been investigated but none of them has been focused on quadcopters.
In this article, a robust adaptive observer algorithm is investigated to show the reliability and accuracy of FD under time-varying faults and external disturbances. Then, we use the Lyapunov theory to verify the stability of system. Finally, an LMI algorithm is applied to obtain designed matrices and parameters and to relax the proposed algorithm.

2. System Description

Figure 1 shows the geometry of the quadcopter, including the placements of motors and propellers. While motors 3 and 4 rotate clockwise, motors 1 and 2 rotate counter-clockwise.

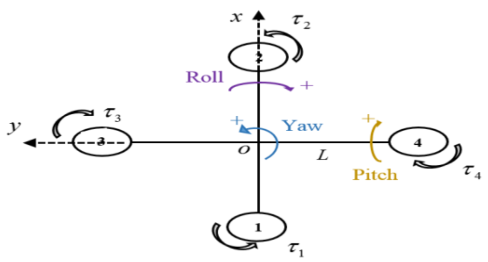

Figure 1: Geometry of the quadcopter.

The four control inputs are presented as

$$\begin{cases} U_1 = F_1 + F_2 + F_3 + F_4 \\ U_2 = (F_3 - F_4)L \\ U_3 = (F_1 - F_2)L \\ U_4 = \tau_1 + \tau_2 - \tau_3 - \tau_4 \end{cases} \quad (1)$$

where τ_i represents the torque of the ith motor; L is arm length; F_i represents the thrust force of the ith propeller; U_1 is total thrust while U_2, U_3, U_4 are the torques in the ϕ, θ and ψ directions.
Thrust force and torque exhibit the following relationships with the rotational speed of the propeller:

$$F_i = k_{th}\Omega_i^2 \tag{2}$$

$$\tau_i = k_d\Omega_i^2 \tag{3}$$

where k_{th} and k_d are the thrust and drag coefficients; Ω_i is the rotational speed of the ith motor.
Substituting equations (2) and (3) in (1) yields

$$\begin{cases} U_1 = k_{th}(\Omega_1^2 + \Omega_2^2 + \Omega_3^2 + \Omega_4^2) \\ U_2 = k_{th}(\Omega_3^2 - \Omega_4^2)L \\ U_3 = k_{th}(\Omega_1^2 - \Omega_2^2)L \\ U_4 = k_d(\Omega_1^2 + \Omega_2^2 - \Omega_3^2 - \Omega_4^2) \end{cases} \tag{4}$$

In previous study[7], the dynamic quadcopter model has been investigated as follows:

$$\begin{cases} I_x\ddot{\phi} = U_2 + (I_y - I_z)\dot{\theta}\dot{\psi} - J_T\dot{\theta}\Omega - K_\phi\dot{\phi} \\ I_y\ddot{\theta} = U_3 + (I_z - I_x)\dot{\phi}\dot{\psi} - J_T\dot{\phi}\Omega - K_\theta\dot{\theta} \\ I_z\ddot{\psi} = U_4 + (I_x - I_y)\dot{\theta}\dot{\phi} - K_\psi\dot{\psi} \end{cases} \tag{5}$$

where I_x, I_y and I_z are the moments of inertia; K_ϕ, K_θ and K_ψ represent drag coefficients; J_T is the rotor inertia; and $\Omega = \Omega_3 + \Omega_4 - \Omega_1 - \Omega_2$.
The state equation has a form as:

$$\begin{cases} \dot{x}(t) = Ax(t) + Bu(t) + \rho(x,u) \\ y = Cx(t) \end{cases} \tag{6}$$

with the state vector $x^T = [\phi\ \theta\ \psi\ \dot{\phi}\dot{\theta}\dot{\psi}]$, the control input vector$u^T = [U_2U_3U_4]$, and the output vector$y^T = [\phi\ \theta\ \psi\ \dot{\phi}\dot{\theta}\dot{\psi}]$.
Because the drag terms are small in flight, they can be considered as disturbances. For simplicity, matrices of state equation (6) can be described as

$$A = \begin{bmatrix} 0&0&0&1&0&0 \\ 0&0&0&0&1&0 \\ 0&0&0&0&0&1 \\ 0&0&0&0&0&0 \\ 0&0&0&0&0&0 \\ 0&0&0&0&0&0 \end{bmatrix} C = \begin{bmatrix} 1&0&0&0&0&0 \\ 0&1&0&0&0&0 \\ 0&0&1&0&0&0 \\ 0&0&0&1&0&0 \\ 0&0&0&0&1&0 \\ 0&0&0&0&0&1 \end{bmatrix}$$

$$B = \begin{bmatrix} 0&0&0 \\ 0&0&0 \\ 0&0&0 \\ \frac{1}{I_x}&0&0 \\ 0&\frac{1}{I_y}&0 \\ 0&0&\frac{1}{I_z} \end{bmatrix} \quad \rho(x,u) = \begin{bmatrix} 0 \\ 0 \\ 0 \\ \frac{(I_y - I_z)\dot{\theta}\dot{\psi} - J_T\dot{\theta}\Omega}{I_x} \\ \frac{(I_z - I_x)\dot{\phi}\dot{\psi} - J_T\dot{\phi}\Omega}{I_y} \\ \frac{(I_x - I_y)\dot{\theta}\dot{\phi}}{I_z} \end{bmatrix}$$

3. Robust Fault Diagnosis Scheme

3.1. An Adaptive Sliding Mode Observer for Fault Diagnosis

The equation (6) can be rewritten in full state space model as

$$\begin{cases} \dot{x}(t) = Ax(t) + Bu(t) + E_d d_1(t) + Fb(t) + \rho(x,u) \\ y = Cx(t) \end{cases} \tag{7}$$

where $y(t) \in R^p$ is the output vectors; $x(t) \in R^n$ represent the state vector; A, B, C, E_d and F are real matrices with proper dimensions; $u(t) \in R^m$ is control input; $d_1(t) \in R^k, b(t) \in R^l$ are the bounded unknown disturbance, and actuator fault.
Before the method is presented, we state the following conditions and lemmas for fault diagnosis[9]:
C1 $(C, A)$is observable.
C2 $\rho(x,u)$ is assumed to be differentiable continuously and Lipschitz with a constant γ, i.e.,$\|\rho(x_1(t),u(t)) - \rho(x_2(t),u(t))\| \le \gamma\|x_1 - x_2\|$.
C3 $b(t)$ and$\dot{b}(t)$ are norm bounded, i.e.,$\|b(t)\| \le b_1, \|\dot{b}(t)\| \le b_2$.
C4 the unknown disturbance is bounded, i.e., $\|d_1(t)\| \le N$where$N$is an unknown constant.
Lemma 1 [10] For given a symmetric matrix $P \ge 0$ and a scalar $\mu \ge 0$, then the inequality holds

$$2x^Ty \le \frac{1}{\mu}x^TPx + \mu y^TP^{-1}y$$

Lemma 2 If the condition C2 satisfies, there exists a matrix $P \ge 0$ such that

$$2e^TP\big(\rho(x_1,u) - \rho(x_2,u)\big) \le \gamma^2e^TPPe + e^Te$$

If all conditions and lemmas hold, the adaptive sliding mode observer is constructed as

$$\begin{cases} \dot{\hat{x}}(t) = A\hat{x}(t) + Bu(t) + E_dh(t) + F\hat{b}(t) + \rho(\hat{x},u) \\ \qquad +K(\hat{y}(t) - y(t)) \\ \hat{y} = C\hat{x}(t) \end{cases} \tag{8}$$

where $\hat{y}(t) \in R^p$ is the observer output vector; $\hat{x}(t) \in R^n$ is the observer state vector; $\hat{b}(t) \in R^l$ is the fault estimation of $b(t)$; K is the observer gain matrix which satisfies that $A - KC$ is a stable matrix; $h(t)$is obtained by following algorithm:

$$\begin{aligned} \dot{z}(t) &= \alpha\|F_1e_y(t)\| \\ h(t) &= -z(t)F_1e_y(t)/\|F_1e_y(t)\| \end{aligned} \tag{9}$$

where α is a positive constant, and F_1will be discussed in the next section.

3.2 Stability

Denote

$$\begin{aligned} e_x &= \hat{x}(t) - x(t) \\ \tilde{z}(t) &= z(t) - N \end{aligned} \tag{10}$$

Then, the error dynamics are shown by

$$\dot{e}_x = (A - KC)e_x(t) + Fe_b + E_d(h(t) - d_1(t)) + \rho(\hat{x},u) - \rho(x,u) \tag{11}$$

where $e_b(t) = \hat{b}(t) - b(t)$

Theorem 1 For a given observer gain$K$, if there existmatrices $P = P^T > 0$, $G = G^T > 0$,F_1, and F_2 such that

$$\begin{bmatrix} X & 0 \\ 0 & Y \end{bmatrix} < 0 \tag{12}$$

$$E_d^TP = F_1C \tag{13}$$

$$F^TP = \frac{1}{\sigma}F_2C \tag{14}$$

where σ is a positive constant, $Y = \frac{\sigma+1}{\sigma}G$, and$X = P(A - KC) + (A - KC)^TP + \gamma^2PP + I$,
then the resulting adaptive law is presented as

$$\dot{\hat{b}}(t) = -\Gamma F_2e_y + \sigma\Gamma\hat{b}(t) \tag{15}$$

where Γ is the learning matrix, $\Gamma = \Gamma^T > 0$; $e_y = \hat{y}(t) - y(t)$

Proof. Given the following Lyapunov function

$$V(t) = e_x^T(t)Pe_x(t) + \frac{1}{\sigma}e_b^T(t)\Gamma^{-1}e_b(t) + \tilde{z}^T(t)\alpha^{-1}\tilde{z}(t) \quad (16)$$

The derivative of equation (16) is

$$\begin{aligned}\dot{V}(t) &= \dot{e}_x^T(t)Pe_x(t) + e_x^T(t)P\dot{e}_x(t) + \frac{2}{\sigma}e_b^T(t)\Gamma^{-1}\dot{e}_b(t) + 2\dot{z}(t)\alpha^{-1}\tilde{z}\\ &= e_x^T(t)[P(A-KC) + (A-KC)^TP]e_x(t) + 2e_x^T(t)PE_d\big(h(t) - d_1(t)\big) + 2e_x^T(t)PFe_b(t)\\ &\quad + 2\|F_1e_y(t)\|(z(t) - N) + 2e_x^T(t)P\big(\rho(\hat{x},u) - \rho(x,u)\big)\\ &\quad + \frac{2}{\sigma}e_b^T(t)\Gamma^{-1}\dot{\hat{b}}(t) - \frac{2}{\sigma}e_b^T(t)\Gamma^{-1}\dot{b}(t)\end{aligned} \quad (17)$$

From Theorem 1, Lemma 1, and Lemma 2, we obtain

$$\begin{aligned}&2e_x^T(t)PFe_b(t) + \frac{2}{\sigma}e_b^T(t)\Gamma^{-1}\dot{\hat{b}}(t)\\ &= 2e_x^T(t)PFe_b(t) + \frac{2}{\sigma}e_b^T(t)\Gamma^{-1}\left(-\Gamma F_2e_y + \sigma\Gamma\hat{b}(t)\right)\\ &= 2e_b^T(t)\hat{b}(t)\\ &\le e_b^T(t)Ge_b(t) + \hat{b}^T(t)G^{-1}\hat{b}(t)\\ &\le e_b^T(t)Ge_b(t) + b_1^2\lambda_{max}(G^{-1})\end{aligned} \quad (18)$$

$$\begin{aligned}&2e_x^T(t)PE_d\big(h(t) - d_1(t)\big)\\ &= 2\left(F_1e_y(t)\right)^T\left(-\frac{z(t)F_1e_y(t)}{\|F_1e_y(t)\|} - d_1(t)\right)\\ &< -2\|F_1e_y(t)\|(z(t) - N)\end{aligned} \quad (19)$$

where $\lambda_{max}(.)$ is the maximum eigenvalue.
According to Lemma 1, we achieve

$$\begin{aligned}-\frac{2}{\sigma}e_b^T(t)\Gamma^{-1}\dot{b}(t) &= \frac{2}{\sigma}\left(-e_b^T(t)\right)\left(\Gamma^{-1}\dot{b}(t)\right)\\ &\le \frac{1}{\sigma}\left(e_b^T(t)Ge_b(t) + \dot{b}^T(t)\Gamma^{-1}G^{-1}\Gamma^{-1}\dot{b}(t)\right)\\ &\le \frac{1}{\sigma}\left(e_b^T(t)Ge_b(t) + b_2^2\lambda_{max}\left(\Gamma^{-1}G^{-1}\Gamma^{-1}\right)\right)\end{aligned} \quad (20)$$

And from Lemma 2 we obtain

$$\begin{aligned}&e_x^T(t)[P(A-KC) + (A-KC)^TP]e_x(t) + 2e_x^T(t)P\big(\rho(\hat{x},u) - \rho(x,u)\big)\\ &\le e_x^T(t)[P(A-KC) + (A-KC)^TP + \gamma^2PP + I]e_x(t)\end{aligned} \quad (21)$$

Substituting (18), (19), (20), and (21) into (17) yields

$$\begin{aligned}\dot{V}(t) &= e_x^T(t)[P(A-KC) + (A-KC)^TP + \gamma^2PP + I]e_x(t) + e_b^T(t)Ge_b(t) + b_1^2\lambda_{max}(G^{-1})\\ &\quad + \frac{1}{\sigma}\left(e_b^T(t)Ge_b(t) + b_2^2\lambda_{max}\left(\Gamma^{-1}G^{-1}\Gamma^{-1}\right)\right)\\ \dot{V}(t) &= e_x^T(t)[P(A-KC) + (A-KC)^TP + \gamma^2PP + I]e_x(t) + \frac{\sigma+1}{\sigma}e_b^T(t)Ge_b(t) + \eta\\ &\le \xi^T(t)\Theta\xi(t) + \eta\end{aligned} \quad (22)$$

where $\eta = b_1^2\lambda_{max}(G^{-1}) + \frac{1}{\sigma}b_2^2\lambda_{max}(\Gamma^{-1}G^{-1}\Gamma^{-1})$
and $\xi(t) = [e_x^T(t) \quad e_b^T(t)]$,
$\Theta = \begin{bmatrix} P(A-KC) + (A-KC)^TP + \gamma^2PP + I & 0 \\ 0 & \frac{\sigma+1}{\sigma}G \end{bmatrix}$.
When $\Theta < 0$, it follows that $\dot{V}(t) < 0$ for $\sigma\|\xi(t)\|^2 > \eta$, where $\sigma = \lambda_{min}(-\Theta)$ .Therefore, following the Lyapunov theory[9], $(e_x(t), e_b(t))$converges to a small set.

Remark 1
While solving (12) needs requires use of the LMI technique, there are certain challenges to solving (13) and (14) simultaneously. These can be overcome by transforming equations (13) and (14) into an optimization problem[11]:

$$\begin{bmatrix} \eta_1 I & E_d^TP - F_1C \\ \left(E_d^TP - F_1C\right)^T & \eta_1 I \end{bmatrix} > 0 \quad (23)$$

$$\begin{bmatrix} \eta_2 I & F^TP - \frac{1}{\sigma}F_2C \\ \left(F^TP - \frac{1}{\sigma}F_2C\right)^T & \eta_2 I \end{bmatrix} > 0 \quad (24)$$

Remark 2
The adaptive law of fault estimation exits if the following conditions satisfies[12]:
C5 $rank(CF) = l$ and $rank(CE_d) = p$
C6 $(A, F, C)$and (A, E_d, C)have invariant zeros whichlies in the open left half plane

4. Simulation

The robust fault diagnosis scheme has been verified using the DJI quadrotor with the parameters shown in Table 1. We chose the following matrices for the simulation: $F = B$ and $E_d = [1 \quad 1 \quad 1 \quad 1 \quad 1 \quad 1]^T$. The Condition C2 is easy to obtain with $\gamma = 1.5$ and Remark 2 is also satisfied, which means that the proposed scheme can be applied.

Table 1: Quadrotor parameters

Parameter	Description	Value
L	Arm length	0.225m
b	Thrust coefficient	9.78×10^{-6}Ns^2/rad^2
d	Drag coefficient	1.55×10^{-7}Nms^2/rad^2
m	Mass	2kg
g	Gravity	9.81m/s^2
$I_x; I_y; I_z$	Moments of inertia	$3 \times 10^{-3}; 3 \times 10^{-3}; 5 \times 10^{-3}$kg.m^2
J_r	Rotor inertia	0.28×10^{-5}N.m/rad/s^2

White noise is injected into the system with the power of0.005. The amplitude is saturated between -1and1. The learning matrix $\Gamma = 10^{-3} \times diag(5,5,5)$, observer gain $K = 200 \times I_{6\times6}$, and sampling time $T = 0.001\ s$ are used to simulate the environment. Matrices are obtained from the adaptive sliding mode observer as follows:

$G = 100 \times I_{6\times6}$

$F_1 = [29.35 \quad 29.35 \quad 29.35 \quad 29.35 \quad 29.35 \quad 29.35]$

$$F_2 = \begin{bmatrix} 14.1 & 4.8 & 4.8 & 3.99 & 4.8 & 4.8 \\ 4.5 & 13.1 & 4.5 & 4.5 & 3684 & 4.5 \\ 3 & 3 & 8.8 & 3 & 3 & 2487.5 \end{bmatrix}$$

$$P = \begin{bmatrix} 29.1 & 0.035 & 0.035 & 0.103 & 0.035 & 0.035 \\ 0.035 & 29.1 & 0.035 & 0.035 & 0.103 & 0.035 \\ 0.035 & 0.035 & 29.1 & 0.035 & 0.035 & 0.103 \\ 0.103 & 0.035 & 0.025 & 29.1 & 0.035 & 0.035 \\ 0.035 & 0.103 & 0.035 & 0.035 & 29.1 & 0.035 \\ 0.035 & 0.035 & 0.103 & 0.035 & 0.035 & 29.1 \end{bmatrix}$$

Two cases of actuator fault $b(t) = [b_1(t) \quad b_2(t) \quad b_3(t)]^T$ are presented in this section. The constant actuator fault is created as

$$b_1(t) = \begin{cases} 0 & 0 < t < 15 \\ 1 & 15 < t < 40 \end{cases}$$

$$b_2(t) = 0, b_3(t) = 0$$

and the associated results are presented in Figure 2.
The time variability of actuator fault is created as

$$b_1(t) = \begin{cases} 0 & 0 < t < 10 \\ sin\,(0.5t) & 10 < t < 40 \end{cases}$$

$$b_2(t) = 0, b_3(t) = 0$$

with the results shown in Figure 3.

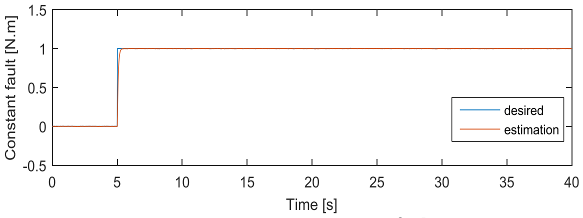

Figure 2: Constant actuator fault

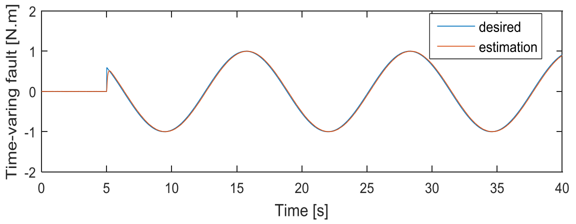

Figure 3: Time variability of actuator fault

In Figure 2, when the fault occurs, the estimation values converge to the desired ones within 0 to 0.5 s. Figure 3 confirms that the proposed scheme is applicable to describe time-varying faults. Because the error term $e_y(t)$ and the actuator fault term $b(t)$ are added in the adaptive algorithm, the fault estimation converges rapidly.

5. Conclusion

In this paper, a nonlinear model of quadrotor in combination with a robust fault diagnosis method has been presented with the actuator fault. Unlike previous works, the method presented here is capable of detecting time-varying faults and solving model uncertainties. The stability of system has been derived using Lyapunov theory. The simulation results could show the benefits of the proposed algorithm. Future studies will focus on FTC controllers to compensate the system faults from fault diagnosis results.

Acknowledgement

This research was supported by the MSIT(Ministry of Science and ICT), Korea, under the ITRC(Information Technology Research Center) support program(IITP-2018-2018-0-01423) supervised by the IITP(Institute for Information & communications Technology Promotion), and also it was partially supported by the National Strategic Project-Fine particle of the National Research Foundation of Korea(NRF) funded by MSIT, ME(Ministry of Environment), and MOHW(Ministry of Health and Welfare) under Grant 2017.

References

[1] Y. Zhang, J. Jiang. Bibliographical review on reconfigurable fault-tolerant control systems. Annu. Rev. Control 32, 229–252 (2008).
[2] A. Freddi, S. Longhi, A. Monteriù. A diagnostic thau observer for a class of unmanned vehicles. J. Intell. Robot. Syst. 67, 1–13 (2012).
[3] F. Chen, W. Lei, G. Tao, B. Jiang. Actuator Fault Estimation and Reconfiguration Control for Quad-rotor Helicopter. International Journal of Advanced Robotic Systems, 13(33), 2016.
[4] L. Ma, Y. M. Zhang. Fault detection and diagnosis for GTM UAV with dual unscented Kalman filter. In: Proc. 2010 AIAA Guidance, Navigation, and Control Conference, pp. 3204–3215.
[5] Z. Cen, H. Noura, T. B. Susilo, Y. A. Youmes. A. Robust Fault Diagnosis for Quadrotor UAVs Using Adaptive Thau Observer. J Intell Robot Syst. 73(1-4), pp. 573-588.
[6] X. Zhang, M. M. Polycarpou, T. Parisini. A robust detection and isolation scheme for abrupt and incipient faults in nonlinear systems. IEEE Trans. Autom. Control, 2002, 47, (4), pp. 576–593.
[7] B. Jiang, M. Staroswiecki, V. Cocquempot. Fault accommodation for nonlinear dynamic systems. IEEE Trans. Autom. Control, 2006, 51, (9), pp. 1578–1583.
[8] B. L. Walcott, M. J. Corless, and S. H. Zak. Comparative study of nonlinear state-observation techniques. Int. J. Control, Vol. 45, No. 6, pp. 2109-2132 (1987).
[9] W. Chen, and M. Saif. Novel sliding mode observers for a class of uncertain systems. American Control Conference (2006).
[10] B. Jiang, J. L. Wang, Y. C. Soh. An adaptive technique for robust diagnosis of faults with independent effects on system outputs. International Journal of Control, Vol. 75(11), 2002, pp. 792-802.
[11] K. Zhang, B. Jiang, and V. Cocquempot. Adaptive observer-based fast fault estimation. Int J. Control, Autom. Syst, Vol. 6, No. 3, pp. 320–326 (2008).
[12] C. Edwards. A comparison of sliding mode and unknown input observers for fault reconstruction. IEEE 43rd Conf. Decis. Control, Vol. 5, pp. 5279–5284 (2004).